Analysis of Nighttime Light Changes and Trends in the 1-Year Anniversary of the Russia–Ukraine Conflict

Lin Wang, Henggang Lei, and Hanqiu Xu

***Abstract*—The Russia–Ukraine conflict has persisted for over a year, posing challenges in assessing and verifying the extent of damage through on-site investigations. Nighttime light (NTL) remote sensing, an emerging approach for studying regional conflicts, can complement traditional methods. This article employs National Aeronautics and Space Administration's Black Marble products to reveal the response characteristics of NTL intensity at national and state scales during the first anniversary of the conflict (January 2022 to February 2023) in Ukraine. The article used the NTL ratio index to assess the relative intensity of NTL and month-on-month change rate, nighttime light change rate index (NLCRI), and the rate (*R* value) of linear regression analysis to depict spatiotemporal dynamics. In addition, Theil–Sen median trend analysis and Mann–Kendall tests were employed to analyze intensity trends, with a "dual-threshold method" to reduce extensive noise interference. The results showed: At the national scale, the conflict resulted in an 84.0% decrease in NTL across Ukraine. At the state scale, the most severe NTL decline occurred near the southwestern border and eastern conflict zone under Ukrainian government control, witnessing over 80% decline rates. The correlation of decreases in NLCRI and *R* values with population displacement, infrastructure damage, or curfew measures demonstrated that the concentration of refugees and electricity facility restoration led to increased NLCRI and *R* values. Overall, NTL reflects critical moments at the national scale and provides insights into military intentions and humanitarian measures at the state scale. Therefore, NTL can effectively serve as a tool for observation and assessment in military conflicts.**

***Index Terms*—Black Marble nighttime lights (NTLs) product suite, multiscale analysis, Russia–Ukraine conflict, spatiotemporal dynamics, VNP46A3 product.**

Manuscript received 9 September 2023; revised 20 November 2023, 25 December 2023, and 19 January 2024; accepted 19 January 2024. Date of publication 23 January 2024; date of current version 6 February 2024. This work was supported in part by the Key Project of The National Natural Science Foundation of China under Grant U2005205, in part by the National Natural Science Foundation of China under Grant 42071300, and in part by the Fujian Province Natural Science Foundation Project under Grant 2023J01417. *(Corresponding author: Hanqiu Xu.)*

Lin Wang and Hanqiu Xu are with the College of Environmental and Safety Engineering, Fujian Provincial Key Laboratory of Remote Sensing of Soil Erosion and Disaster Prevention, Institute of Remote Sensing Information Engineering, Fuzhou University, Fuzhou 350108, China (e-mail: wanglin@fzu.edu.cn; hxu@fzu.edu.cn).

Henggang Lei is with the Academy of Digital China (Fujian), Fujian Provincial Key Laboratory of Remote Sensing of Soil Erosion and Disaster Prevention, Institute of Remote Sensing Information Engineering, Fuzhou University, Fuzhou 350108, China (e-mail: lhg_rs04@163.com).

Digital Object Identifier 10.1109/JSTARS.2024.3357727

I. Introduction

THE Russian–Ukrainian conflict, which began on February 24, 2022, has now been ongoing for over a year. Both sides have been engaged in continuous ground and air combat in Ukraine, resulting in damage to residential areas and severe destruction of power facilities and other infrastructure, leading to widespread power and water shortages within Ukraine [1].

Tracking and investigating the impact of armed conflicts is essential for reducing conflict risks and providing humanitarian assistance to local populations. However, the prolonged conflict has made it difficult to conduct on-site investigations and verifications of the extent of destruction in the conflict zone. With the development of satellite technology, using remote sensing data for real-time monitoring of armed conflicts has become a cost-effective, rapid, and efficient approach [2].

Nighttime light (NTL) remote sensing is an optical remote sensing technology that can detect faint NTLs. It can provide information that is not obtainable by daytime remote sensing and reflect changes in human activities from a unique perspective. The occurrence and persistence of conflicts often cause large-scale damage to buildings and infrastructure, seriously affecting regional energy supply and socioeconomic activities. In addition, conflicts often lead to the departure of a significant number of residents from the affected area, leading to a significant reduction in the local population. This decline in population and social activities contributes to the decrease and attenuation of artificial light sources at night, which can be reflected in the NTL images. Therefore, it can macroscopically reflect the extent of war destruction [3]. The changes in artificial light radiation on the ground before and after the war can reflect the variations in human activities, power supply, and other conditions to a certain extent, making it an effective method for studying conflict zones using remote sensing. In the 21st century, especially in the past decade, NTL remote sensing has been used in military conflicts, such as the South Ossetia War [4], the Syrian crisis [5], and the Yemeni Civil War [6], providing a new source of information for observing war dynamics, assessing regional destruction, and facilitating humanitarian aid.

After extensive research, NTL remote sensing has made significant progress in data acquisition, processing, and applications [7], [8], [9]. Currently, the most widely used NTL remote sensing data in the world are from the Defense Meteorological Satellite Program Operational Line Scan System (DMSP-OLS)

TABLE I
BLACK MARBLE PRODUCT SUITE

<table>
<tr><th>Product suite</th><th>Type</th><th>Content</th><th>Temporal resolution</th></tr>
<tr><td>VNP46A1</td><td>at-sensor TOA NTL product</td><td>26 layers (sensor radiance, zenith and azimuth angles at-sensor, solar, and lunar, cloud mask flag, time, shortwave IR radiance, brightness temperatures, VIIRS quality flags, moon phase angle, and moon illumination fraction)</td><td>1 day</td></tr>
<tr><td>VNP46A2</td><td>Moonlight and atmosphere-corrected NTL product</td><td>7 layers [BRDF-corrected NTL, gap-filled BRDF-corrected NTL, lunar irradiance, mandatory quality flag, latest high-quality retrieval (number of days), snow flag, and cloud mask flag</td><td>1 day</td></tr>
<tr><td>VNP46A3</td><td rowspan="2">Composite product (moonlight and atmosphere-corrected)</td><td rowspan="2">28 layers (NTL composite, the number of observations, quality, and standard deviation for multiview zenith angle categories (near-nadir, off-nadir, and all angles) and snow status (snow-covered and snow-free) as well as land water mask, platform, latitude, and longitude)</td><td>1 month</td></tr>
<tr><td>VNP46A4</td><td>1 year</td></tr>
</table>

and Suomi National Polar-Orbiting Partnership Visible Infrared Imaging Radiometer Suite (NPP-VIIRS) [10]. DMSP-OLS is the longest running NTL remote sensing satellite, providing data from 1992 to 2013. Subsequently, National Oceanic and Atmospheric Administration (NOAA) released a new generation of NPP-VIIRS NTL remote sensing data, which started providing data in 2012. Compared to DMSP-OLS, NPP-VIIRS has shown improvements in performance, including increased spatial resolution, better radiance detection capability, and reduced saturation in urban areas, indicating its greater potential in various applications [11], [12].

Using NPP-VIIRS data, National Aeronautics and Space Administration (NASA) has further developed the Black Marble product suite, providing cloud-free images that have been corrected for atmospheric, terrain, lunar BRDF, thermal, and straylight effects [13]. The Black Marble product suite includes the following four datasets (Table I). The VNP46A1 dataset contains sensor data and other data needed for correction. The VNP46A2 dataset is the daily scale data, correcting the VNP46A1 data for atmosphere and moonlight. The VNP46A3 dataset consists of synthetic monthly data. The VNP46A4 dataset includes synthetic data on an annual scale. Both VNP46A3 and VNP46A4 contain synthetic data without zenith angle position and snow cover state. This NTL product suite provides higher quality data for monitoring short-term and long-term changes related to human activities [7], [14], [15].

Currently, researchers have used NTL remote sensing to investigate the Russia–Ukraine conflict. For example, Zheng et al. [7] used the Black Marble daily product (VNP46A2) to study the level of energy shortage in Ukraine and the affected population within three weeks after the outbreak of the conflict (until March 17, 2022). Huang et al. [16] established a linear model using the Black Marble daily and annual products (VNP46A2 and VNP46A4) in conjunction with partial refugee data from the United Nations Refugee Agency to quantify and evaluate the changes in refugee movements within ten weeks after the outbreak of the conflict (until May 2, 2022). Yu et al. [17] used the Black Marble daily product (VNP46A2) to study the spatiotemporal dynamics of NTLs in Ukraine during the period until October 14, 2022, following the outbreak of the conflict. However, due to data gaps in the summer, the authors did not analyze the dynamics from May to August. These studies objectively reflect the impact of the Russia–Ukraine conflict from different perspectives but have mostly focused on a limited time range within the first several months after the onset of the conflict, primarily during the more intense periods in spring and summer [7], [16], [17]. However, in order to comprehensively track and analyze the situation changes during the year-long confrontation and stalemate in the conflict, to continuously assess the response characteristics of NTL data to changes in the conflict situation, relying solely on samples from the intense conflict periods is insufficient. In addition, Black Marble products occasionally exhibit large-scale high-intensity background noise, and the magnitude of the noise values is strongly positively correlated with brightness radiance values. This positive correlation directly affects the denoising effect, and the conventional threshold processing methods cannot achieve satisfactory results. Previous articles either did not address this issue [17], or did not evaluate and discuss the denoising effect and solutions to this problem [7], [16], [18], [19], [20]. Furthermore, due to the poor image quality of NPP-VIIRS in the high-latitude regions of the Northern Hemisphere during the summer, the corrected Black Marble data cannot completely cover the study area in Ukraine, leading to data gaps in time-series studies. However, similar existing studies did not address this issue.

In view of this, this article period covers a full year of the conflict (until the second winter after the outbreak of the conflict), covering multiple stages of the conflict, allowing us to continuously assess the response characteristics of the total NTL intensity to the overall situation, military intentions of both sides, and humanitarian measures throughout the long-lasting conflict. The article also explores methods to remove background noise from the data product and its effects, as well as how to minimize and mitigate the impact of data gaps on the analysis of military

Fig. 1. Location map of study area.

conflict temporal trends. The research results are expected to provide a new perspective and valuable reference data for monitoring situation changes in the military conflict and assessing their impact.

II. Materials and Methods

A. Study Area and Study Period

Ukraine is located in Eastern Europe, along the northern coasts of the Black Sea and the Sea of Azov. It shares borders with Russia and Belarus to the east and north, and Poland, Slovakia, and Hungary to the west. It also borders Romania and Moldova to the south. With a total area of 603 550 km^2, Ukraine is the second-largest country in Europe, with a population of 43.5 million [21]. The country is divided into 27 primary administrative regions, including 24 states, one autonomous republic (Crimean Republic), and two cities with special status (Kyiv and Sevastopol). Since Crimean Republic and Sevastopol were minimally affected by the conflict, they were not included in the scope of this article (Fig. 1).

The study period for this article spans from January 2022, before the conflict outbreak, to February 2023, marking the 1-year anniversary of the conflict [22]. The overall process is divided into four stages: conflict outbreak stage (January 2022–March 2022), easing situation stage (April 2022–August 2022), counter-offensive stage (September 2022–October 2022), and confrontation stage (November 2022–February 2023).

B. Data Sources

1) Nighttime Light Images: This article aims to use statistical analysis of NTL variations to monitor and evaluate the situational characteristics of different phases within the 12 months after the conflict outbreak. The impacts of conflict events often persist for a certain period of time. Therefore, the monthly composite product VNP46A3 is better suited to meet our requirements. VNP46A3 is generated from daily atmospherically and lunar-BRDF-corrected NTL radiance to remove the influence of extraneous artifacts and biases. The data consist of 28 layers, including information on NTL composite, the number of observations, quality, standard deviation for multiview zenith angle categories, snow status, as well as land water mask, platform, latitude, and longitude [13].

Due to poor image quality of NPP-VIIRS in the high-latitude regions of the Northern Hemisphere during summer, the corrected Black Marble data for June and July 2022 could not fully cover the study area (Fig. 2). Therefore, these missing data were not included in subsequent research.

2) Auxiliary Data: The vector data of Ukraine's national boundaries and administrative boundaries are sourced from Natural Earth's Global Boundary Vector Data (https://www.naturalearthdata.com/features/).

C. Methods

1) Denoising Method for VNP46A3 Images: VNP46A3 data contain extensive irregular noise, and the magnitude of the noise values is strongly positively correlated with the brightness radiance values [7], [23]. This positive correlation directly impacts the denoising effectiveness, and conventional thresholding methods do not yield satisfactory results. For example, a low denoising threshold cannot completely eliminate noise, resulting in images filled with noise dots, while a high denoising threshold would remove useful regions with lower light brightness.

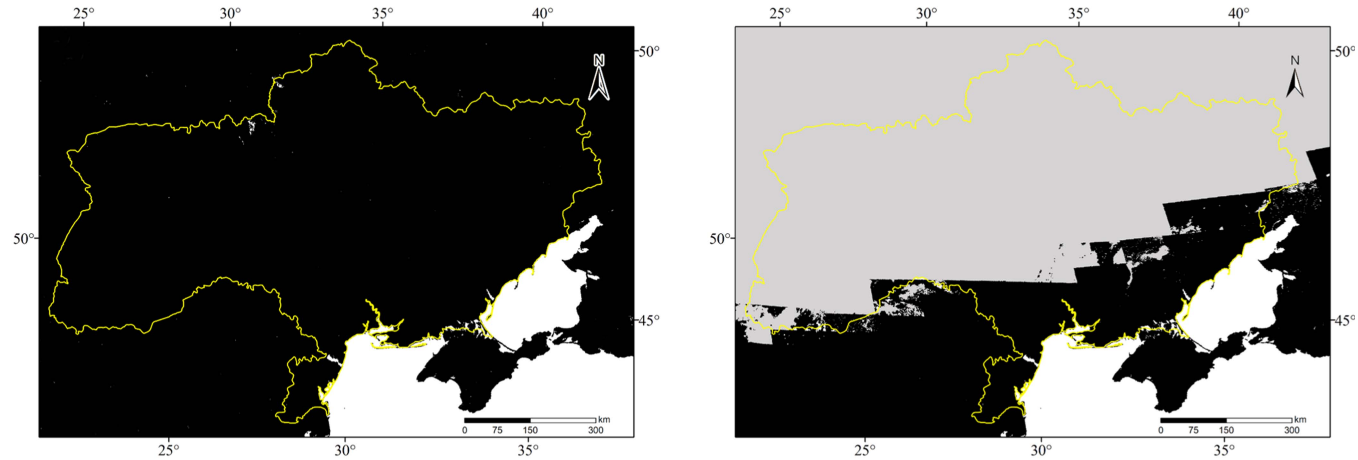

(a) (b)

Fig. 2. Examples of original nighttime light remote sensing images in the study area. (a) April data (complete coverage). (b) June data (incomplete coverage).

To address this issue, we adopted a “dual-threshold method” for denoising processing. The specific procedure is as follows: 1) for the January image, we used 1 nWatts/cm^2/sr [16] as the denoising threshold to identify the regions of effective NTL brightness before conflict occurred and created a mask for the NTL background brightness; and 2) using this mask, we processed the other postconflict images one by one, employing 0.5 nWatts/cm^2/sr [18] as the denoising threshold, thus completing the noise processing procedure.

2) National-Scale Analysis: To represent the total NTL intensity in different periods of Ukraine, we used the nighttime light ratio index (NLRI) [14]. This index compares the NTL values of each month with the NTL value of January (preconflict).

In addition, we used the month-on-month change rate (MoM) of NTL intensity to visually highlight the monthly variations in NTLs. The formulas for NLRI and MoM are as follows:

$$\text{NLRI} = \frac{\text{NTL}i}{\text{NTL}1} \tag{1}$$

$$\text{MoM} = \frac{\text{NTL}i - \text{NTL}i - 1}{\text{NTL}i - 1} \tag{2}$$

where NTL_1 is the NTL intensity in January, and NTL_i is the NTL intensity in the *i*th month.

We conducted Theil–Sen median trend analysis and Mann–Kendall tests on the time-series images within the study period to analyze the trend of NTL intensity in the study area. This trend analysis method exhibits high tolerance for outliers and missing values [9], [24], [25], making it more suitable for the time-series analysis in this article. The formula for Theil–Sen median trend analysis is as follows:

$$\text{Slope} = \text{median}\left(\frac{\text{NTL}i - \text{NTL}j}{j - i}\right) \tag{3}$$

where NTL_i and NTL_j are the NTL intensity of the *i*th and *j*th months, and Slope is the slope of data change. When Slope $>$ 0, it indicates an increasing trend in NTL intensity, while Slope $<$ 0 indicates a decreasing trend.

The formula for the Mann–Kendall test is as follows:

$$Z = \begin{cases} (S-1)/\sqrt{\text{Var}(S)} & \text{if} \quad S > 0 \\ 0 & \\ (S+1)/\sqrt{\text{Var}(S)} & \text{if} \quad S < 0 \end{cases} \tag{4}$$

$$S = \sum_{i=1}^{n-1} \sum_{j=i+1}^{n} \text{sgn}\left(\text{NTL}j - \text{NTL}i\right) \tag{5}$$

$$\text{sgn}\left(\text{NTL}i - \text{NTL}j\right) = \begin{cases} +1 & \text{if} \quad \text{NTL}j - \text{NTL}i > 0 \\ 0 & \text{if} \quad \text{NTL}j - \text{NTL}i = 0 \\ -1 & \text{if} \quad \text{NTL}j - \text{NTL}i < 0 \end{cases} \tag{6}$$

$$\text{Var}\left(S\right) = n\left(n-1\right)\left(2n+5\right)/18 \tag{7}$$

where *n* is the number of months under study, *Z* is the test statistic value, *S* is the sum of the positive and negative trends in the sample data, and sgn is the sign function. When $|Z| < 1.96$, it indicates an insignificant trend, while $|Z| > 1.96$ indicates a significant trend.

3) State-Scale Analysis: Based on the timeline of the Russia–Ukraine conflict divided into four stages, we conducted linear regression analysis on the light intensity of different states during each stage to obtain the rate *R*, which represents the rate of change in light intensity for the corresponding state during that stage. The formula is as follows:

$$R = \frac{\sum_{i=1}^{n} xi\text{NTL}i - n\bar{x}\overline{\text{NTL}}}{\sum_{i=1}^{n} xi^2 - n\bar{x}^2} \tag{8}$$

where *n* is the time sequence of the study, x_i is the month value, NTL_i is the monthly NTL intensity, $\bar{x}$ is the average value of the month, and $\overline{\text{NTL}}$ represents the average NTL intensity as the initial light levels of each state before the conflict were not the same, to demonstrate the impact of changing military situation on the NTL intensity of different states, we used the nighttime light change rate index (NLCRI) to represent the relative degree of change in monthly NTL intensity for each state [26]. The

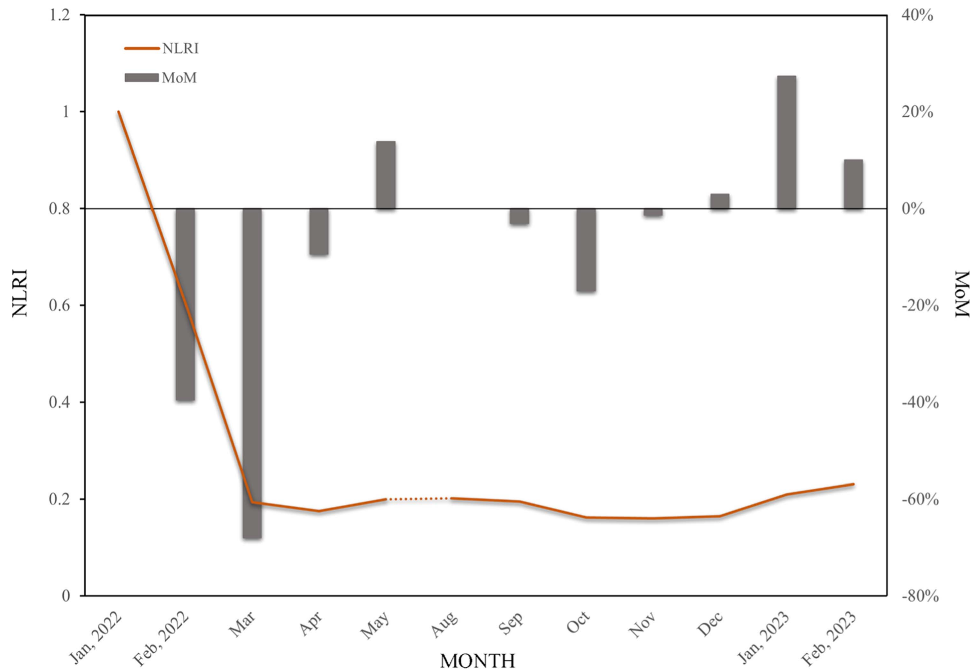

Fig. 3. Statistics of nighttime light changes in Ukraine (January 2022–February 2023).

formula is as follows:

$$\mathrm{NLCRI} = \frac{\mathrm{NTL}i - \mathrm{NTL}i - 1}{\mathrm{NTL1}} \quad (9)$$

where NTL_i is the monthly NTL intensity. Compared with the MoM of light intensity, NLCRI eliminates the influence of preconflict light levels in each state and can better reflect the regions with significant fluctuations in light intensity during different stages of the conflict.

III. Results

A. National-Scale Analysis of Nighttime Light Changes

The NLRI and MoM of the conflict (January 2022–February 2023) were calculated and statistics of NTL changes (Fig. 3) were plotted.

From Fig. 3, it can be observed that following Russia's military operation in Ukraine on February 24, 2022, the NTL intensity in Ukraine significantly decreased, reaching two low points in March–April 2022 and September–October 2022. These two phases corresponded to periods of attacks initiated by both Russia and Ukraine, characterized by missile and artillery strikes and rapidly changing front lines. The month of March experienced the most significant MoM value decrease in NTL intensity (−68.0%) due to the massive population displacement, destruction of urban facilities, and the implementation of curfews in Ukraine resulting from outbreak of the conflict. In April, the focus of the Russian attacks shifted, leading to a stalemate between both sides. The eastern region, particularly the Donbass area, remained the main conflict zone, while the western region was more affected by airstrikes and policy restrictions. As a result, although the total NTL intensity tended to stabilize or even slightly recover, the recovery rate was slow. The NLRI decreased again in September and October when Ukraine launched counterattacks, reaching a value below 0.2 in September and hitting a new low of 0.160 in October. During this period, Ukraine suffered multiple rounds of large-scale airstrikes targeting its power facilities, resulting in severe damage to the power system. The situation gradually changed starting from November. Based on the MoM values, the NTL intensity shifted from a decrease to a continuous increase. Furthermore, the NLRI value reached its highest point (0.231) in February 2023, after the outbreak of the conflict. However, the light intensity remained significantly lower than before the conflict.

TABLE II
Nighttime Light Changes in Ukraine (January 2022–February 2023)

Changes in quantity	Value
The maximum change of NLRI (%)	−84.0
Area of significant reduction (km^2)	6230.75
Area of reduction (km^2)	3860.25

The trend of NTL changes in Ukraine throughout the entire time period was obtained using Theil–Sen analysis and Mann–Kendall test. A graph illustrating the trend of changes (Fig. 4) and a corresponding table (Table II) were created.

From Table II and Fig. 4, it can be seen that the conflict resulted in an 84.0% decrease in NTL intensity across Ukraine, with a total area of NTL decrease reaching 1.01×10^4 km^2. All regions within Ukraine experienced varying degrees of NTL decrease.

The areas with large cities as the core witnessed more significant decreases, with the most severe decreases occurring in the states of Kharkiv (85.4%), Sumy (83.4%), and Chernihiv (83.2%). Other administrative regions with a decrease rate

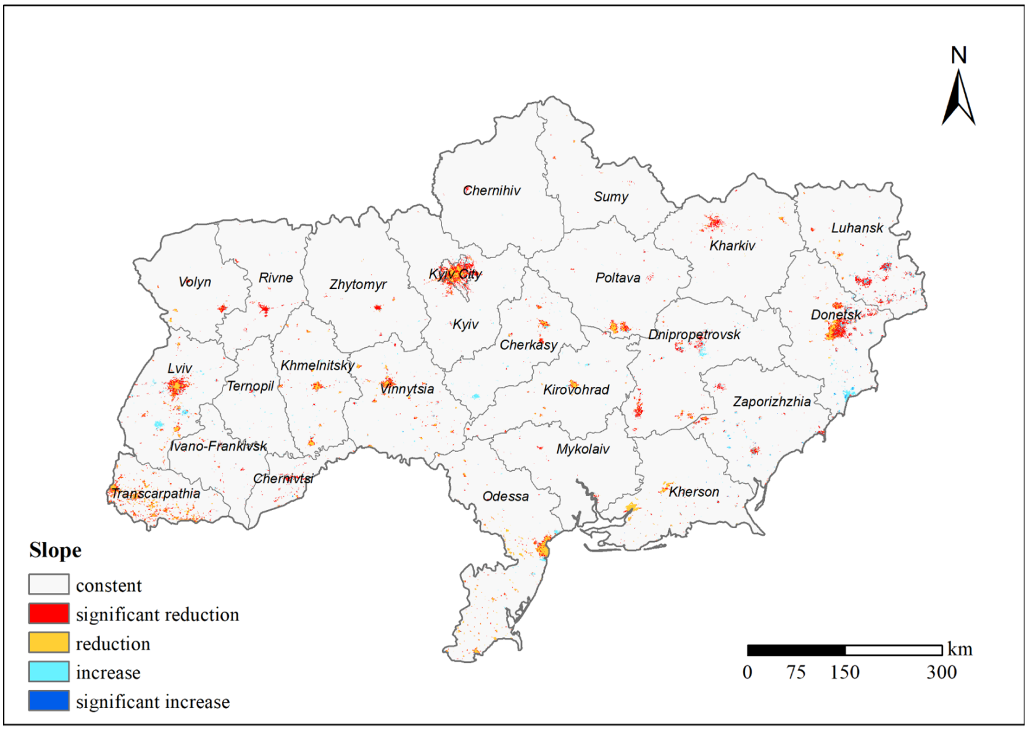

Fig. 4. Trend of nighttime light changes in Ukraine (January 2022–February 2023).

TABLE III
STATISTICS OF NIGHTTIME LIGHT CHANGES IN EACH STATE OF UKRAINE (JANUARY 2022–MARCH 2022)

Region	R	NLCRI (%)		Region	R	NLCRI (%)	
		Feb.	Mar.			Feb.	Mar.
Mykolaiv	−0.490	−26.2	−71.8	Zaporizhzhia	−0.415	−43.4	−39.7
Ternopil	−0.486	−38.5	−58.6	Kyiv City	−0.403	−51.2	−29.4
Ivano-Frankivsk	−0.485	−43.9	−53.0	Donetsk	−0.389	−51.2	−26.6
Dnipropetrovsk	−0.478	−30.2	−65.4	Volyn	−0.388	−42.9	−34.7
Kharkiv	−0.468	−64.7	−28.9	Poltava	−0.385	−41.6	−35.3
Zhytomyr	−0.466	−38.9	−54.2	Odessa	−0.335	−19.2	−47.8
Chernihiv	−0.464	−48.5	−44.12	Lviv	−0.335	−29.8	−37.1
Sumy	−0.458	−56.3	−35.3	Vinnytsia	−0.297	−20.5	−38.9
Chernivtsi	−0.455	−23.2	−67.9	Khmelnitsky	−0.295	−20.7	−38.2
Rivne	−0.453	−45.2	−45.3	Luhansk	−0.256	−40.3	−11.0
Kyiv	−0.424	−49.0	−35.9	Kherson	−0.247	−20.3	−29.2
Cherkasy	−0.421	−20.1	−64.1	Transcarpathia	−0.187	−18.1	−19.3
Kirovohrad	−0.417	−34.7	−48.6				

exceeding 80% were mainly concentrated in the eastern conflict zone controlled by Ukraine and the southwestern border region.

B. State-Scale Analysis of Nighttime Light Changes

1) Conflict Outbreak (January 2022–March 2022): In this stage, Russia deployed ground forces from the north (Kyiv direction), northeast (Sumy–Kharkiv direction), east (Donbas direction), and south (Kherson direction) to rapidly advance into internal areas of Ukraine. At the same time, the Russian Air Force conducted air strikes in coordination with the Rocket Forces on military facilities, such as suburban airports in multiple states of Ukraine.

By using the statistical data of NTL intensity in each state of Ukraine from January to March 2022, R and NLCRI values were obtained (Table III, Fig. 5).

It can be observed that the large-scale military operations by the Russian side had significant impacts on Ukraine during this stage. Two distinct clusters with noticeable changes in R values (deep red areas in Fig. 5) were located in the eastern and western parts of Ukraine. The eastern cluster was situated along the direction of the Russian ground forces' advance, including Mykolaiv (−0.490) and Dnipropetrovsk (−0.478), while the western cluster was located near the Ukrainian border and far from the center of conflict zone, such as Ternopil (−0.486) and Ivano–Frankivsk (−0.485).

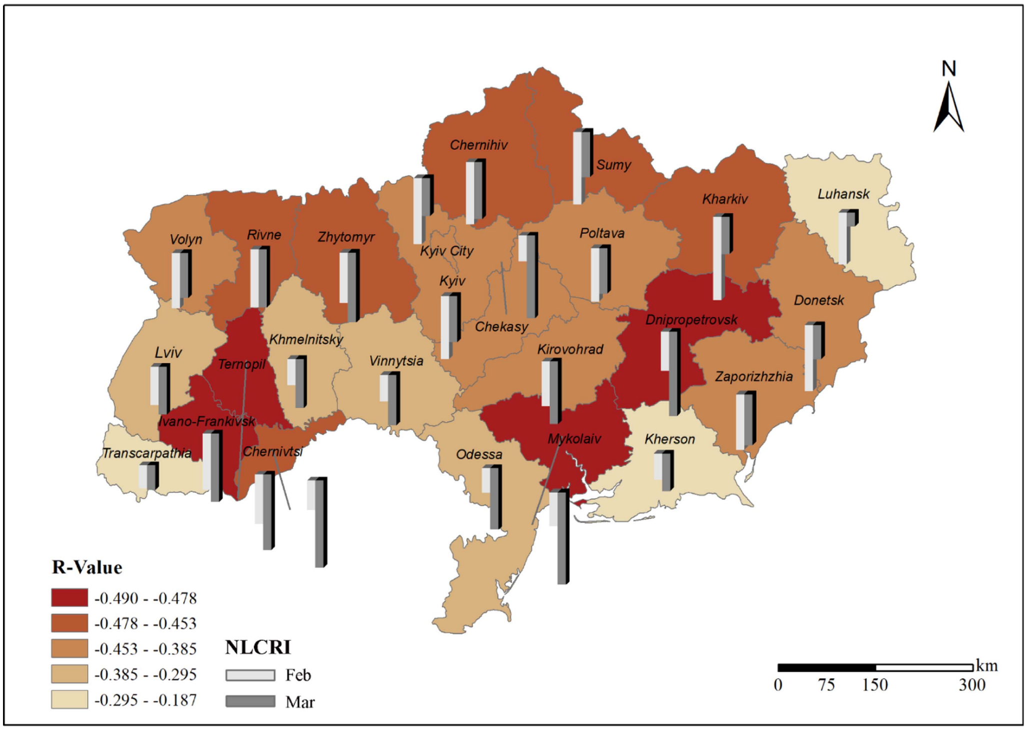

Fig. 5. Nighttime light changes in each state of Ukraine (January 2022–March 2022).

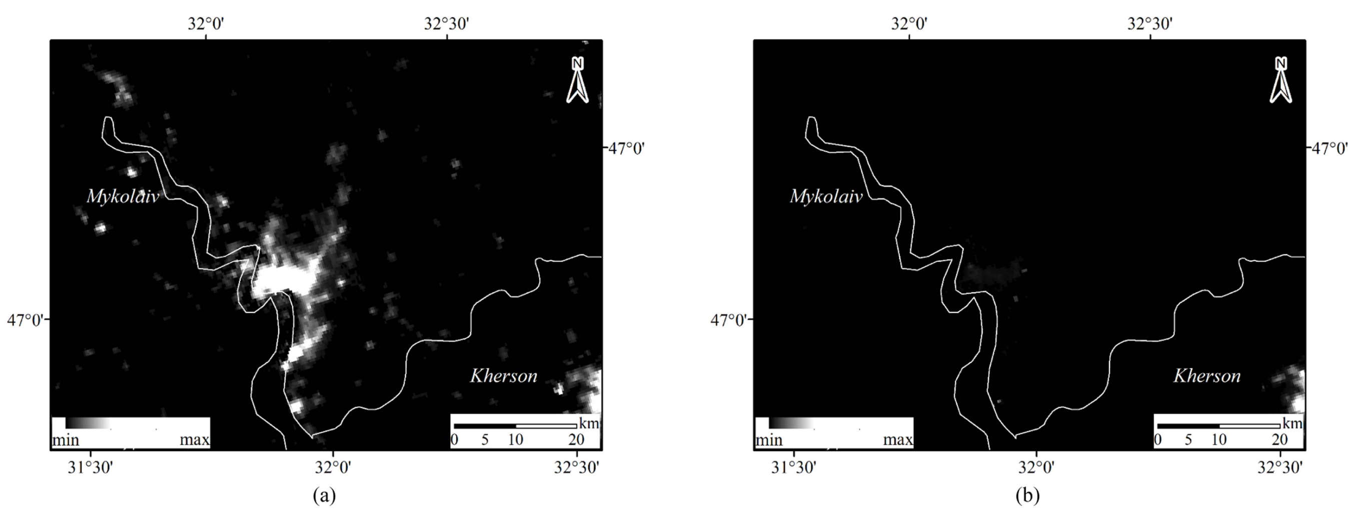

Fig. 6. Nighttime light images of Mykolaiv state. (a) January 2022. (b) March 2022.

NLCRI values also exhibited significant changes. Due to the sudden advancement of the Russian forces, there was a substantial decrease in NTL intensity at the end of February in several states along the eastern and northern borders of Ukraine. March witnessed the largest scale and fast advancement of Russian ground forces, resulting in even greater declines in NTL intensity in nonborder states in eastern Ukraine and various western states. The NTL intensity in states like Dnipropetrovsk and Mykolaiv dropped to less than 5% of the preconflict levels. Fig. 6 illustrates the dramatic changes in NTL intensity in the southern border region of Mykolaiv state before and after the conflict.

In summary, it can be inferred that the main reasons for the rapid decrease in NTL intensity in several western border states were due to displaced residents and restrictions on nighttime electricity usage by urban residents. Meanwhile, military attacks, damage to infrastructure and energy facilities, as well as curfews, were the primary factors contributing to the decline in light intensity in the eastern conflict zone [27], [28], [29].

It is worth noting that there were certain states along the border where NTL intensity declined slowly (light red areas in Fig. 5), such as Luhansk in the east, Kherson in the south, and Transcarpathia in the west. Considering the information about the conflict, it can be inferred that during this stage, multiple

TABLE IV
STATISTICS OF NIGHTTIME LIGHT CHANGES IN EACH STATE OF UKRAINE (APRIL 2022–AUGUST 2022)

Region	R	NLCRI (%)				
		Apr	May	Jun	Jul	Aug
Volyn	0.181	−3.4	12.6	NULL	NULL	NULL
Rivne	0.061	−1.0	29.6	NULL	NULL	NULL
Chernivtsi	0.013	0.2	8.7	NULL	NULL	3.5
Ternopil	0.012	−0.5	2.9	NULL	NULL	5.4
Transcarpathia	0.010	−1.2	4.9	NULL	NULL	−17.1
Khmelnitsky	0.010	−4.3	4.3	NULL	NULL	−2.0
Ivano-Frankivsk	0.008	0.1	3.6	NULL	NULL	2.8
Zhytomyr	0.007	−3.5	1.0	NULL	NULL	NULL
Lviv	0.007	−1.6	3.4	NULL	NULL	1.0
Donetsk	0.006	−2.6	3.0	NULL	NULL	0.6
Zaporizhzhia	0.006	2.0	3.7	NULL	NULL	0.9
Cherkasy	0.005	1.0	−0.4	NULL	NULL	1.0
Mykolaiv	0.004	1.4	0.5	NULL	NULL	−0.8
Dnipropetrovsk	0.003	−1.0	1.6	NULL	NULL	3.3
Kharkiv	0.002	−4.5	1.1	NULL	NULL	4.6
Kyiv City	0.002	−1.5	1.9	NULL	NULL	NULL
Kyiv	0.001	−1.0	1.2	NULL	NULL	NULL
Kirovohrad	0.000	−0.6	−1.0	NULL	NULL	3.8
Chernihiv	−0.002	−4.5	0.2	NULL	NULL	NULL
Sumy	−0.002	−3.0	−2.7	NULL	NULL	NULL
Vinnytsia	−0.003	−4.4	1.3	NULL	NULL	0.1
Odessa	−0.005	−0.7	0.4	NULL	NULL	−0.4
Poltava	−0.009	−1.4	−0.3	NULL	NULL	0.8
Kherson	−0.011	−1.0	0.1	1.4	−3.3	−3.9
Luhansk	−0.015	−13.4	6.5	NULL	NULL	5.5

rounds of negotiations took place between Russia and Ukraine, providing evacuation channels and timeframes for Ukrainian civilians. Several border states, including the aforementioned three states, were administrative areas through which refugees needed to pass [30], [31], [32]. This might explain the slow decline in NTL intensity in these regions.

2) Easing Situation (April 2022–August 2022): During this stage, Russia began adjusting its strategic objectives in April, and the focus of both sides gradually shifted to the eastern region of Ukraine, where a stalemate ensued. Table IV and Fig. 7 present the statistical data of *R* and NLCRI values in each state from April to August 2022.

Based on the *R* values, it can be observed that the downward trend in NTL intensity slowed down in most states, and some states even experienced a slight recovery in light intensity.

This feature is further illustrated by NLCRI values. Several states in northern and eastern Ukraine experienced a decline in light intensity in April but started to show an increase from May onwards. Taking Luhansk as an example, the NLCRI value was −13.4% in April, the lowest in the country, but it reached 6.5% in May, ranking fourth nationwide.

Reportedly, a considerable number of displaced residents returned to Ukraine during this stage, enabling reconstruction efforts and normal functioning in various states [33], [34]. This might explain the relatively rapid recovery of NTL intensity in several western states, such as Volyn and Rivne. Fig. 8 demonstrates the recovery of NTL intensity in the central area of Rivne state during this stage.

3) Counter Offense (September 2022–October 2022): During this stage, the Ukrainian army launched a major attack from the Kharkiv direction at the end of August, causing the Russian army to lose control over parts of Kharkiv and Donetsk. After the Russian retreat, martial law was imposed in their controlled areas.

Using the statistical data on NTL intensity in each state in Ukraine from September to October 2022, we obtained the values of *R* and NLCRI (Table V, Fig. 9).

Based on the *R* values, it can be observed that the NTL intensity in most Ukrainian states decreased during this stage, with a significant decline in several northeastern states due to the Ukrainian counter offensive. The NLCRI indicates that during September, states such as Kharkiv, Luhansk, and Donetsk in the northeast of Ukraine experienced a considerable decline.

Luhansk, in particular, witnessed an 11.7% decrease in NTL intensity.

In October, the Russian army conducted multiple rounds of aerial strikes on energy and power facilities within Ukraine, leading to the implementation of rotational power outages in different regions [35], [36]. This became the primary cause for the overall decline in NTL intensity across states during that month. Fig. 10 illustrates the decline in NTL intensity in the central region of Kirovohrad state.

4) Confrontation (November 2022–December 2023): The ground-based counterattack by Ukraine essentially concluded in early November, marking the re-entry of both sides into a

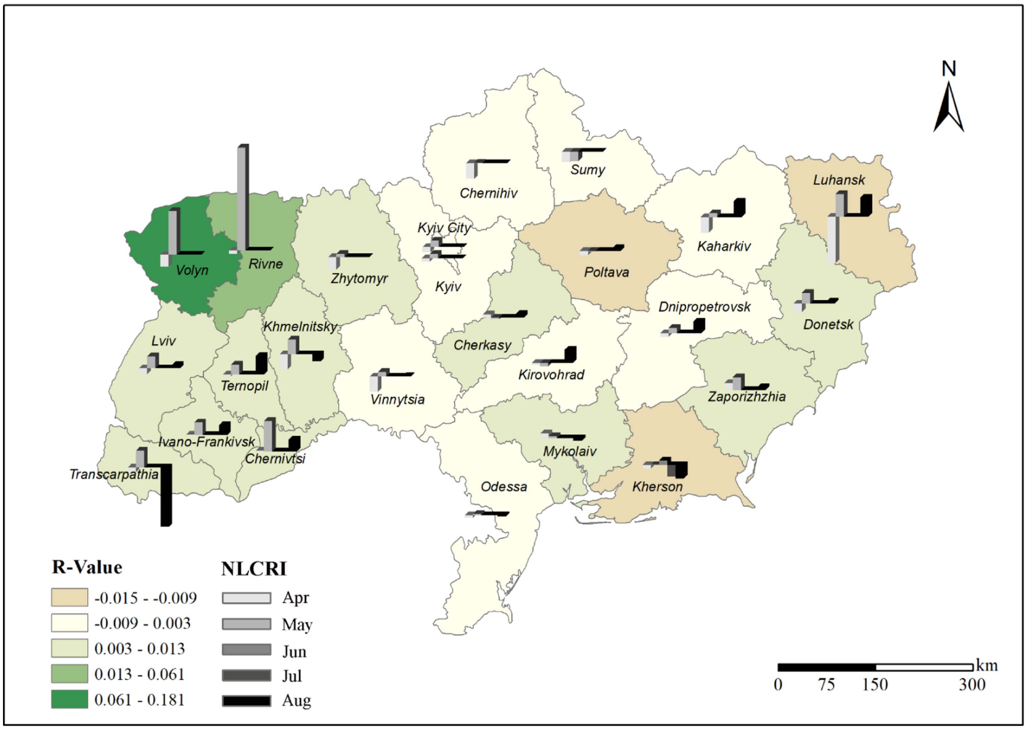

Fig. 7. Nighttime light changes in each state of Ukraine (April 2022–August 2022).

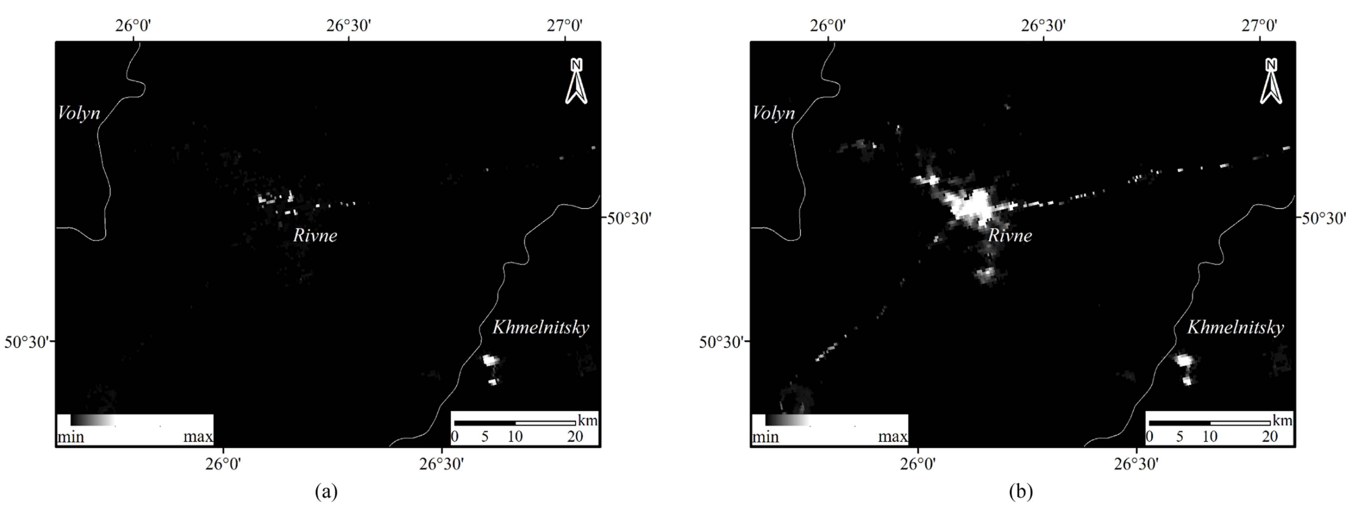

Fig. 8. Nighttime light images of Rivne state. (a) April 2022. (b) August 2022.

confrontational state during this stage. By using the statistical data on NTL intensity in each state in Ukraine from November 2022 to February 2023, we obtained the values of *R* and NLCRI (Table VI, Fig. 11).

From the *R* value, it can be observed that during this stage, NTL intensity gradually recovered in most regions across the country, especially in the eastern region under Russian control where the recovery was relatively fast.

However, some states in the western Ukrainian-controlled area still experienced a continuous decline in NTL intensity, primarily concentrated in states with a significant number of energy facilities, such as Rivne, Khmelnitsky, Mykolaiv, and states with larger populations, such as Odessa, Kyiv, and Dnipropetrovsk. It is presumed that this is related to the continuous attacks by the Russian side on power and energy facilities within Ukraine during this stage. The changes in NLCRI indicate that the NTL intensity in most states started to increase after entering 2023, reaching the highest level of recovery since the outbreak of the conflict. However, overall, there is still a significant gap in the total NTL intensity compared to before the conflict. Fig. 12 demonstrates the recovery of NTL intensity in the southern region of Luhansk state before and after entering 2023.

TABLE V
STATISTICS OF NIGHTTIME LIGHT CHANGES IN EACH STATE OF UKRAINE (SEPTEMBER 2022–OCTOBER 2022)

Region	R	NLCRI (%)		Region	R	NLCRI (%)	
		Sep.	Oct.			Sep.	Oct.
Transcarpathia	−0.062	−8.6	−3.9	Lviv	−0.023	2.8	−7.5
Luhansk	−0.057	−11.7	0.2	Sumy	−0.023	−1.7	−2.8
Poltava	−0.040	−5.4	−2.7	Rivne	−0.017	4.7	−8.1
Volyn	−0.039	−5.6	−2.3	Ivano-Frankivsk	−0.016	−3.3	−1.6
Vinnytsia	−0.038	1.0	−8.6	Cherkasy	−0.014	2.4	−5.2
Chernivtsi	−0.036	2.3	−9.5	Chernihiv	−0.013	−0.5	−2.1
Kirovohrad	−0.036	−0.7	−6.6	Zaporizhzhia	−0.013	−2.5	−0.2
Donetsk	−0.034	−5.4	−1.5	Dnipropetrovsk	−0.013	−2.8	0.2
Khmelnitsky	−0.032	1.1	−7.5	Mykolaiv	−0.012	−1.7	−0.7
Kharkiv	−0.029	−5.1	−0.7	Kyiv	−0.008	5.2	−6.8
Ternopil	−0.028	0.5	−6.0	Kherson	−0.008	2.7	−4.3
Kyiv City	−0.024	2.9	−7.0	Odessa	0.014	2.6	0.3
Zhytomyr	−0.023	0.8	−5.3				

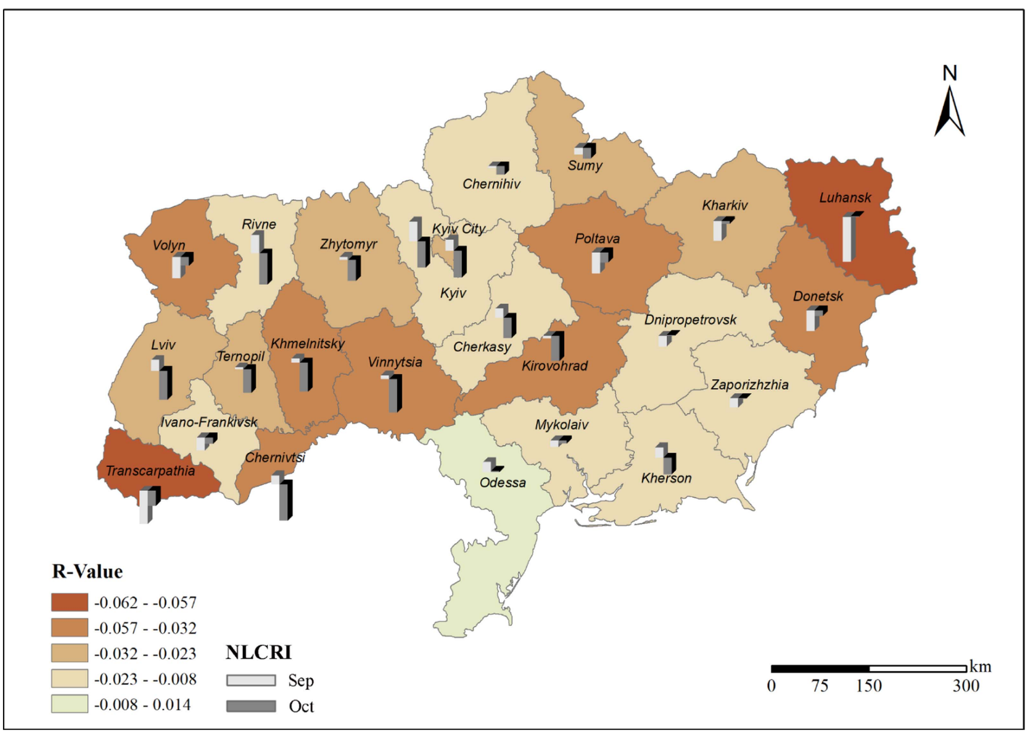

Fig. 9. Nighttime light changes in each state of Ukraine (September 2022–October 2022).

IV. DISCUSSION

A. Denoising Effect of "Dual Threshold Method"

As mentioned earlier, sporadic and extensive high-intensity background noise is an unavoidable issue in the Black Marble products. In order to verify whether the image noise is caused by the correction, we have tried to remove the noise via pseudo invariant features (PIF) calibration. We proceeded to select a number of unaffected urban areas outside the study area (Chisinau, Moldova; Istanbul, Turkey; Sofia, Bulgaria; Bucharest, Romania; and Debrecen, Hungary) and calculated their NLRI values before and after PIF calibration (Fig. 13). It became evident that these areas showed similar NLRI values before and after the calibration, all hovering around a value of 1, and their NLRI values remain largely stable, relative to the conflict-affected Ukraine. This indicated that the NTL changes are real on the ground rather than the calibration problem with the imagery, and PIF calibration may not reduce the extensive noise interference present in the imagery.

Although threshold-based denoising is a conventional approach, it usually employed the "single threshold" denoising

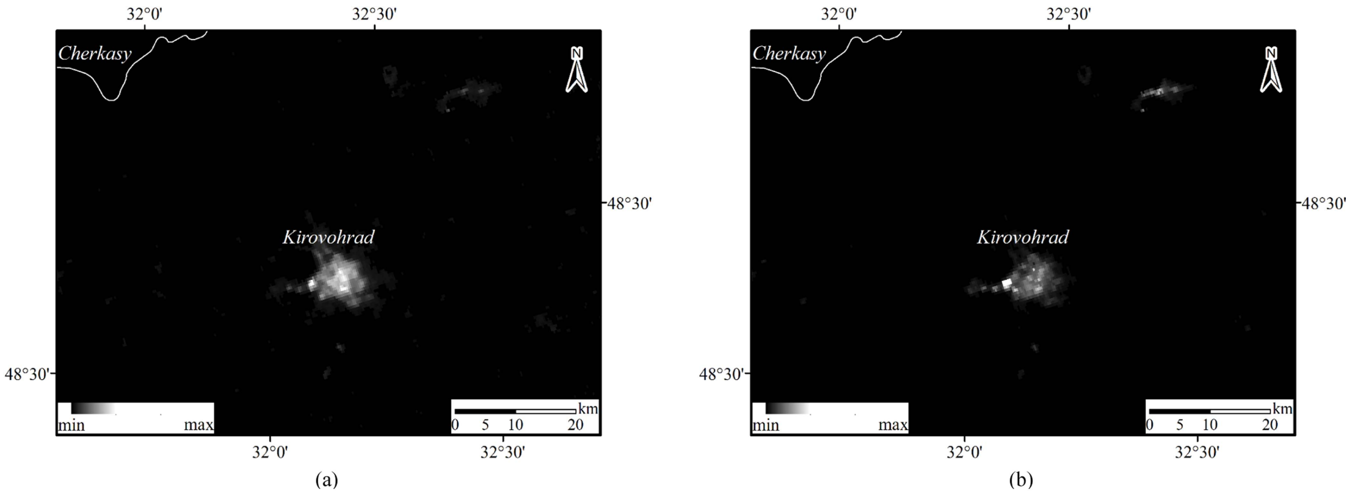

Fig. 10. Nighttime light images of Kirovohrad state. (a) August 2022. (b) October 2022.

TABLE VI
STATISTICS OF NIGHTTIME LIGHT CHANGES IN EACH STATE OF UKRAINE (NOVEMBER 2022–FEBRUARY 2023)

Region	**R**	**NLCRI (%)**			
		Nov.	**Dec.**	**Jan. 2023**	**Feb. 2023**
Luhansk	0.096	0.8	7.1	14.1	15.7
Cherkasy	0.070	5.8	13.5	−3.6	14.1
Chernivtsi	0.055	6.1	−4.3	14.3	6.5
Donetsk	0.047	−0.8	4.5	6.8	7.2
Zhytomyr	0.039	7.3	2.1	3.9	3.0
Ternopil	0.039	5.6	−1.8	14.1	−5.2
Poltava	0.033	2.9	−0.8	10.5	−1.1
Ivano-Frankivsk	0.032	4.4	1.0	8.9	−3.3
Zaporizhzhia	0.029	0.9	3.9	7.0	−2.6
Kharkiv	0.028	1.2	2.4	8.8	−4.2
Vinnytsia	0.026	0.8	−13.6	13.3	12.5
Kirovohrad	0.026	7.0	2.5	3.8	−3.3
Dnipropetrovsk	0.022	1.9	3.7	4.3	−3.0
Mykolaiv	0.018	2.5	11.2	−0.6	−9.3
Chernihiv	0.012	3.8	−0.7	3.0	−1.5
Lviv	0.011	−0.9	0.5	5.4	−2.3
Sumy	0.011	2.7	1.9	1.8	−2.7
Kyiv	0.000	−0.8	−2.2	−0.2	4.5
Kyiv City	−0.008	−2.7	−1.8	−0.9	2.5
Transcarpathia	−0.014	−14.2	−6.3	4.3	10.1
Khmelnitsky	−0.017	−13.6	−5.1	4.3	6.1
Volyn	−0.023	−1.0	−7.8	−1.8	3.8
Odessa	−0.031	−5.9	−8.6	0.9	2.0
Rivne	−0.043	−16.3	6.9	−10.4	0.3
Kherson	−0.053	−3.5	−12.3	−1.2	−2.9

method to reduce background noise of the Black Marble products. We used the "dual threshold method" for noise reduction during the preprocessing of the original images to reduce the interference of image noise on regional statistics. In order to demonstrate the difference in denoising effects between the "dual threshold method" and the traditional single threshold method, we applied three different threshold methods to the original image time series and plotted the NLRI comparison chart (Fig. 14).

From Fig. 14, we can observe the following.

1) The results obtained using a low denoising threshold (0.5 nWatts/cm^2/sr) show the greatest difference compared to the other two methods. The NLRI value in January 2023 is even nearly 280% higher than that of the dual threshold method. The reason is that the overall brightness of the image in January 2023 is high, and due to the positive correlation between noise and brightness, the noise level in the image is also high. If a low denoising threshold is

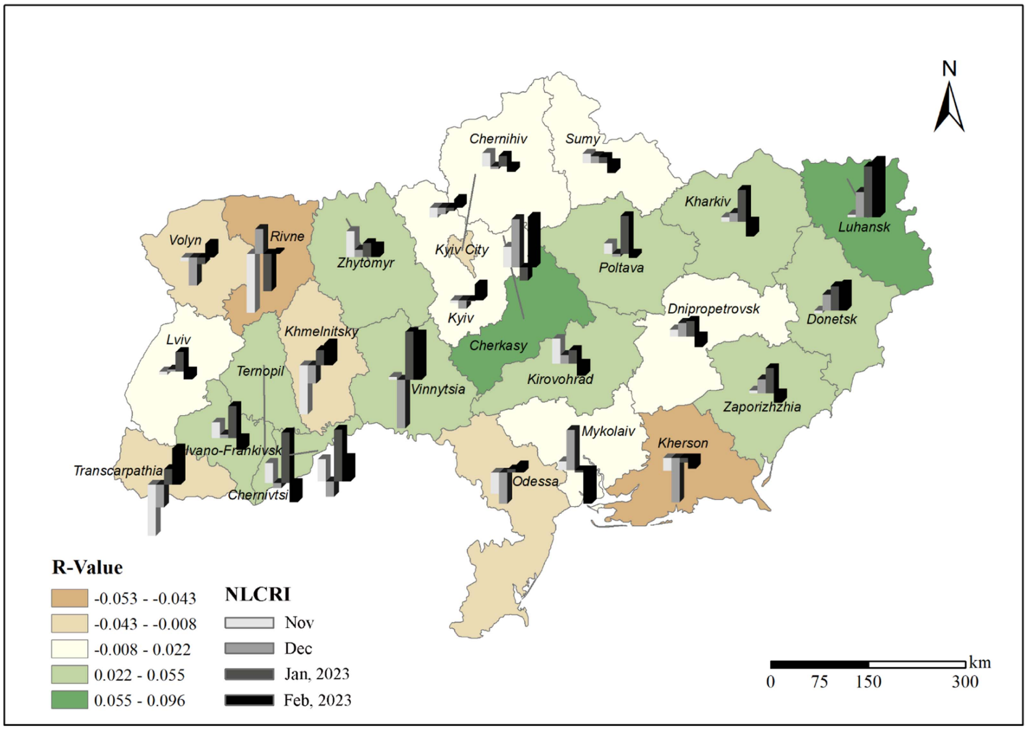

Fig. 11. Nighttime light changes in each state of Ukraine (November 2022–February 2023).

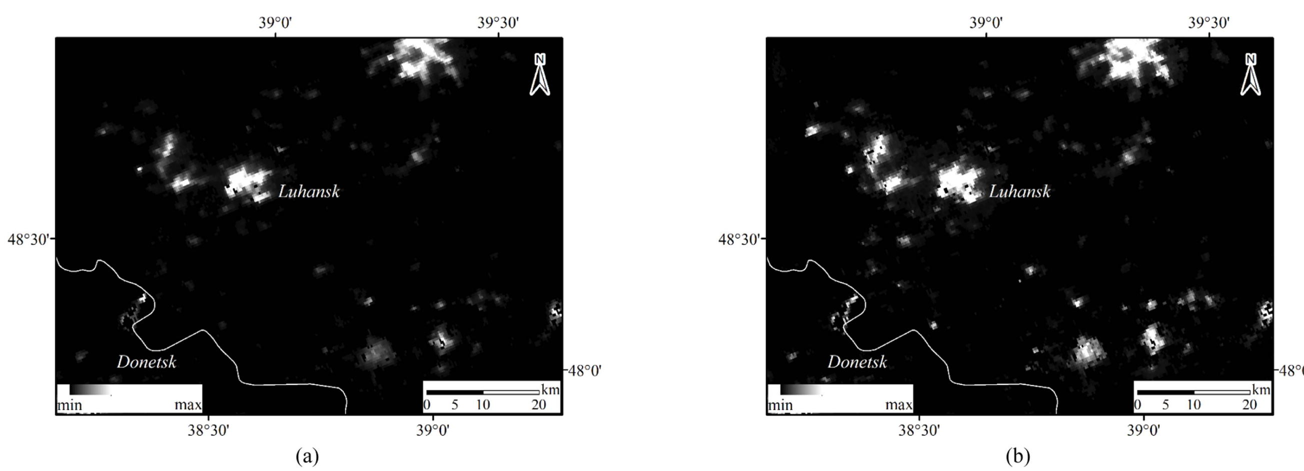

Fig. 12. Nighttime light images of Luhansk state. (a) November 2022. (b) February 2023.

used, it will leave behind a significant amount of high-value noise, resulting in abnormally high NLRI values. Fig. 15 demonstrates this phenomenon using the results of processing Chernihiv state in that month.

The results obtained using a high denoising threshold (1 nWatts/cm^2/sr) show a similar trend to the dual threshold method, but with lower intensity, averaging only 70% of the results obtained with the dual threshold method. This is mainly because some valid pixels with lower light intensity values are removed by the high threshold. Fig. 15(c) presents this phenomenon using the results of processing Chernihiv state in January 2023. Therefore, the "dual threshold method" proposed in this article can effectively address this problem and achieve better results than conventional single-threshold denoising methods.

B. Response Characteristics of Nighttime Light Images to the Russia–Ukraine Conflict

Based on our analysis, we believe that Black Marble's VNP46A3 monthly composite product shows a good and timely response to the Russia–Ukraine conflict, as follows:

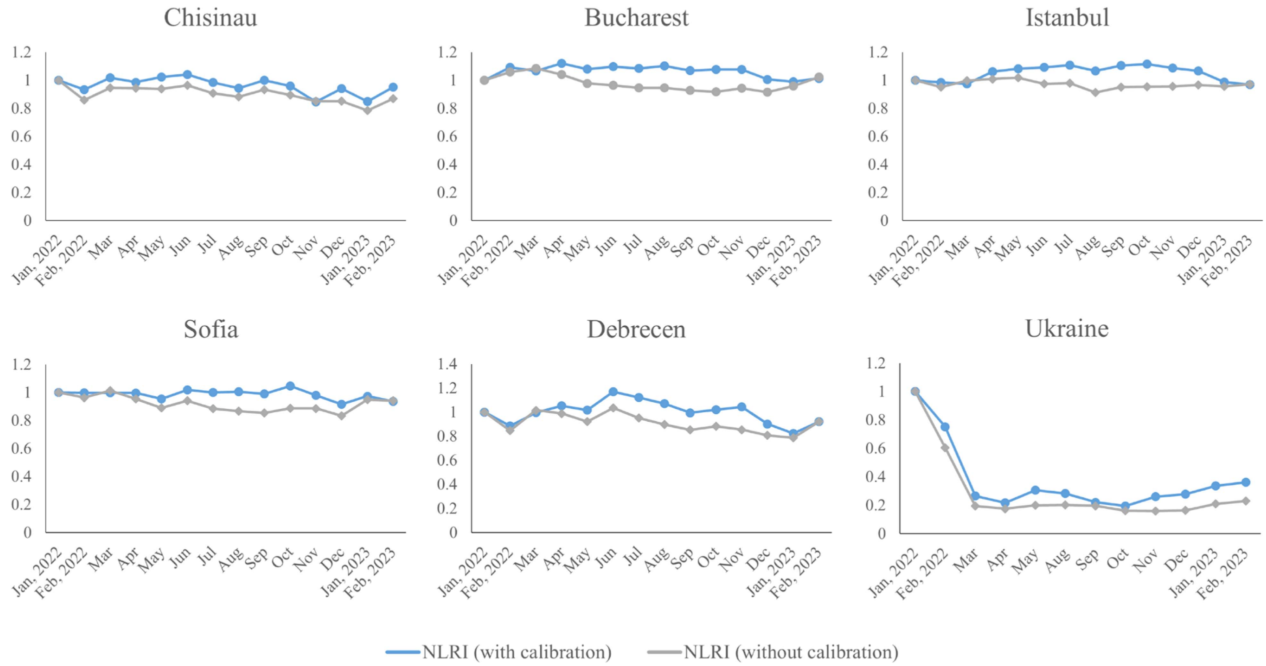

Fig. 13. Nighttime light changes in the reference group (November 2022–February 2023).

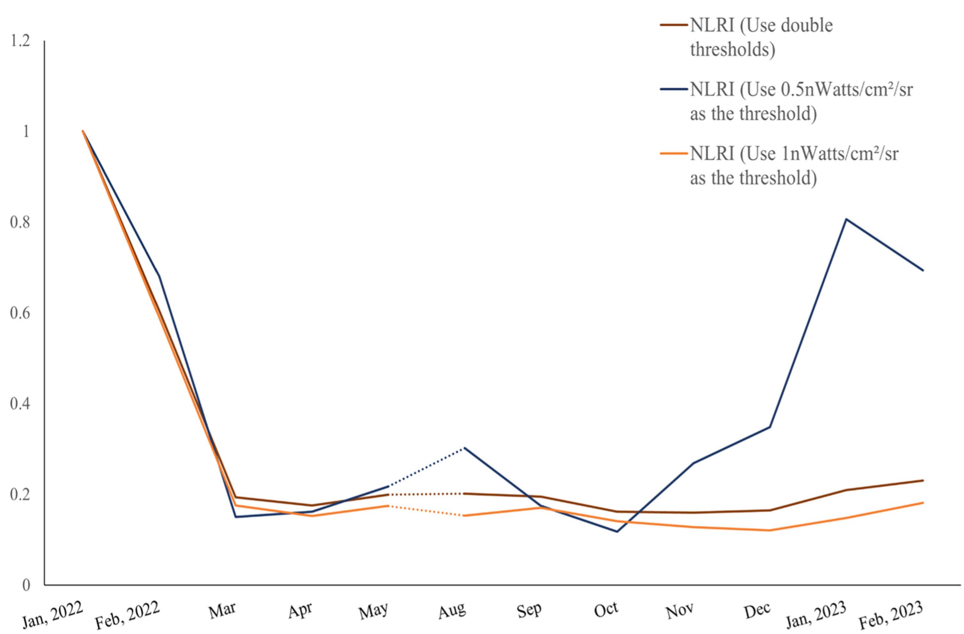

Fig. 14. Variation of NLRI with different threshold selections.

1) The overall NTL intensity in Ukraine reflects the impact of the conflict. As mentioned earlier, military conflicts typically result in damage to buildings and infrastructure, insufficient energy supply, and a significant loss of population, leading to a decrease in the NTL intensity. From the start of the conflict up until the study period on February 28, 2023, the monthly NTL intensity in Ukraine decreased significantly, even failing to reach 25% of the preconflict level. The maximum decrease in monthly lights intensity was 84.0%.
2) At a national scale, the NLRI and MoM of NTLs reflect the changes in the conflict situation, such as outbreak, easing situation, counter-offense, and confrontation. For example, when the Russia–Ukraine conflict broke out in February 2022, the MoM in March dropped to its lowest point of the year at −68.0%. In April, as the

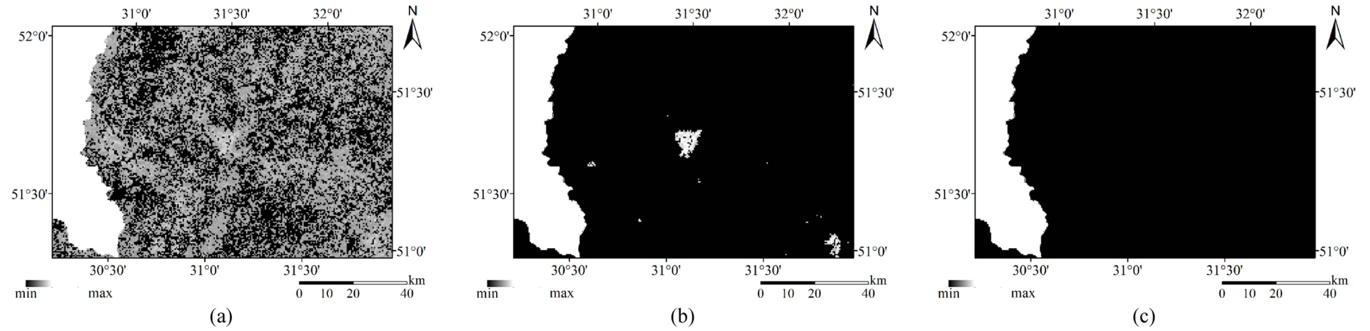

Fig. 15. Nighttime light images of Chernihiv (January 2023): (a) result with low denoising threshold, (b) result with dual thresholds, and (c) result with high denoising threshold.

Russian side shifted its offensive focus and both sides entered a stalemate phase, the MoM rose to 13.8% in May, and the NLRI reached 0.199. When Ukraine launched a comprehensive counteroffensive in October, the NLRI in November dropped to its lowest point of the year at 0.160 (Fig. 3). The conflict caused a significant population exodus, infrastructure damage, and curfew policies, which reduced the overall NTL intensity and led to decreases in NLRI and MoM. Conversely, localized ceasefires, refugee returns, and repairs to electricity and other infrastructure have contributed to their recovery.

3) At a state scale, the NLCRI and S values of NTLs reflect the military intentions and humanitarian measures of the conflicting parties. For example, during the conflict outbreak stage, low values of NLCRI and S appeared in states, such as Mykolaiv and Dnipropetrovsk in eastern Ukraine, which were the main combat areas during this stage, indicating the primary direction of advance for Russian ground forces. At the same time, high values of NLCRI and R appeared in states, such as Luhansk, Kherson, and Transcarpathia, which were designated as refugee evacuation corridors according to the Russian–Ukrainian negotiations, reflecting the humanitarian achievements of the talks during this stage. Similarly, during the confrontation stage, low values of NLCRI and R were concentrated in states, such as Rivne, Khmelnitsky, and Mykolaiv, where there were more energy infrastructure facilities, indicating the Russian military's intention to "destroy power and energy facilities" through airstrikes. As mentioned before, the population exodus and infrastructure damage caused by military clashes significantly reduced the NTL intensity, resulting in decreased NLCRI and R values. Conversely, the concentration of refugees and the corresponding restoration of electricity facilities and support have greatly mitigated the decrease in NLCRI and R values during the conflict.

V. Conclusion

Since the outbreak of the Russia–Ukraine conflict, both sides have engaged in prolonged clashes and standoffs in Ukraine. Using NTL remote sensing data, the impact of the conflict during the first year was monitored and analyzed. The main conclusions are as follows.

1) The "dual threshold method" effectively removes widespread irregular noise in the Black Marble data, improving image quality. Using Theil–Sen median trend analysis and Mann–Kendall tests mitigates the negative effects of missing NTL data on trend analysis.
2) In the absence of on-site investigations, NTLs provide an objective reflection of the overall impact of the Russia–Ukraine conflict across Ukraine. Throughout the first year of the conflict, nationwide NTL intensity has decreased by up to 84.0%, with NTL intensity not even reaching 25% of preconflict levels. Kharkov, Sumy, and Chernihiv are the three administrative regions with the largest decline in NTL intensity, while other regions with more than an 80% decrease are primarily located in the eastern Ukrainian-controlled conflict zone and the southwestern border.
3) NTL data can reflect the intentions of the conflicting parties and the overall situation. The NLRI and MoM of NTLs at the national scale reflect key shifts in the conflict, such as outbreak, easing situation, counter-offense, and confrontation. The NLCRI and R values of NTLs at the state scale reflect the military intentions and humanitarian achievements of the conflicting parties, such as the effectiveness of humanitarian evacuation corridors, the continuation of curfew measures, and the dynamics of energy infrastructure damage or restoration under military strikes. Therefore, NTL data can serve as an effective means for observing and evaluating military conflicts.

References

[1] M. Bogner, "Head of human rights monitoring mission in Ukraine on the situation in Ukraine," Ohchr.ocg, 2022. Accessed: Aug. 31, 2023. [Online]. Available: https://www.ohchr.org/en/statements/2022/03/situation-Ukraine

[2] X. Li, F. Chen, and X. Chen, "Satellite-observed nighttime light variation as evidence for global armed conflicts," *IEEE J. Sel. Top. Appl. Earth Observ. Remote Sens.*, vol. 6, no. 5, pp. 2302–2315, Oct. 2013, doi: 10.1109/JSTARS.2013.2241021.

[3] D. R. Li and X. Li, "Use of night-time light remote sensing in humanitarian disaster evaluation," *Chin. J. Nature*, vol. 40, no. 03, pp. 169–176, 2018.

[4] F. D. W. Witmer and J. O'Loughlin, "Detecting the effects of wars in the Caucasus regions of Russia and Georgia using radiometrically normalized DMSP-OLS nighttime lights imagery," *GISci. Remote Sens.*, vol. 48, no. 4, pp. 478–500, Oct. 2011, doi: 10.2747/1548-1603.48.4.478.

[5] X. Li and D. Li, "Can night-time light images play a role in evaluating the Syrian Crisis?," *Int. J. Remote Sens.*, vol. 35, no. 18, pp. 6648–6661, Sep. 2014, doi: 10.1080/01431161.2014.971469.
[6] W. Jiang, G. He, T. Long, and H. Liu, "Ongoing conflict makes Yemen dark: From the perspective of nighttime light," *Remote Sens.*, vol. 9, no. 8, Aug. 2017, Art. no. 798, doi: 10.3390/rs9080798.
[7] Z. Zheng et al., "Estimates of power shortages and affected populations during the initial period of the Ukrainian–Russian conflict," *Remote Sens.*, vol. 14, no. 19, Sep. 2022, Art. no. 4793, doi: 10.3390/rs14194793.
[8] Z. Zheng, Y. Chen, Z. Wu, X. Ye, G. Guo, and Q. Qian, "The desaturation method of DMSP/OLS nighttime light data based on vector data: Taking the rapidly urbanized China as an example," *Int. J. Geogr. Inf. Sci.*, vol. 33, no. 3, pp. 431–453, Mar. 2019, doi: 10.1080/13658816.2018.1538516.
[9] J. Wu, Z. Wang, W. Li, and J. Peng, "Exploring factors affecting the relationship between light consumption and GDP based on DMSP/OLS nighttime satellite imagery," *Remote Sens. Environ.*, vol. 134, pp. 111–119, Jul. 2013, doi: 10.1016/j.rse.2013.03.001.
[10] K. Shi et al., "Evaluating the ability of NPP-VIIRS nighttime light data to estimate the gross domestic product and the electric power consumption of China at multiple scales: A comparison with DMSP-OLS data," *Remote Sens.*, vol. 6, no. 2, pp. 1705–1724, Feb. 2014, doi: 10.3390/rs6021705.
[11] X. Li, H. Xu, X. Chen, and C. Li, "Potential of NPP-VIIRS nighttime light imagery for modeling the regional economy of China," *Remote Sens.*, vol. 5, no. 6, pp. 3057–3081, Jun. 2013, doi: 10.3390/rs5063057.
[12] K. Shi, C. Huang, B. Yu, B. Yin, Y. Huang, and J. Wu, "Evaluation of NPP-VIIRS night-time light composite data for extracting built-up urban areas," *Remote Sens. Lett.*, vol. 5, no. 4, pp. 358–366, Apr. 2014, doi: 10.1080/2150704X.2014.905728.
[13] M. O. Roman, Z. Wang, R. Shrestha, Y. Tian, and V. Kalb, Black Marble User Guide (Version 1.3), 2022. Accessed: Nov. 3, 2023. [Online]. Available: https://ladsweb.modaps.eosdis.nasa.gov/api/v2/content/archives/Document%20Archive/Science%20Data%20Product%20Documentation/VIIRS_Black_Marble_UG_v1.3_Sep_2022.pdf
[14] Z. Wang, M. O. Román, Q. Sun, A. L. Molthan, L. A. Schultz, and V. L. Kalb, "Monitoring disaster-related power outages using NASA Black Marble nighttime light product," *Int. Arch. Photogrammetry Remote Sens. Spatial Inf. Sci.*, vol. XLII–3, pp. 1853–1856, Apr. 2018, doi: 10.5194/isprs-archives-XLII-3-1853-2018.
[15] G. Xu, T. Xiu, X. Li, X. Liang, and L. Jiao, "Lockdown induced night-time light dynamics during the COVID-19 epidemic in global megacities," *Int. J. Appl. Earth Observ. Geoinf.*, vol. 102, Oct. 2021, Art. no. 102421, doi: 10.1016/j.jag.2021.102421.
[16] C. Huang et al., "Mapping of nighttime light trends and refugee population changes in Ukraine during the Russian–Ukrainian War," *Front. Environ. Sci.*, vol. 11, Jan. 2023, Art. no. 1055100, doi: 10.3389/fenvs.2023.1055100.
[17] Y. Yu, S. Liu, Y. Li, and K. Shi, "Satellite remotely sensed nighttime lights reveal spatiotemporal dynamics of the Ukrainian–Russian conflict," *IEEE Geosci. Remote Sens. Lett.*, vol. 20, Jun. 2023, Art. no. 2503005, doi: 10.1109/LGRS.2023.3290559.
[18] Q. Zheng, Q. Weng, Y. Zhou, and B. Dong, "Impact of temporal compositing on nighttime light data and its applications," *Remote Sens. Environ.*, vol. 274, Jun. 2022, Art. no. 113016, doi: 10.1016/j.rse.2022.113016.
[19] Z. Wang, R. M. Shrestha, M. O. Roman, and V. L. Kalb, "NASA's black marble multiangle nighttime lights temporal composites," *IEEE Geosci. Remote Sens. Lett.*, vol. 19, May 2022, Art. no. 2505105, doi: 10.1109/LGRS.2022.3176616.
[20] T. Li, Z. Zhu, Z. Wang, M. O. Román, V. L. Kalb, and Y. Zhao, "Continuous monitoring of nighttime light changes based on daily NASA's Black Marble product suite," *Remote Sens. Environ.*, vol. 282, Dec. 2022, Art. no. 113269, doi: 10.1016/j.rse.2022.113269.
[21] "Ukraine country profile," BBC.com, 2023. Accessed: Aug. 31, 2023. [Online]. Available: https://www.bbc.com/news/world-Europe-18018002
[22] D. Hao and H. Kong, China. After one year of the Russian-Ukrainian conflict, what four stages can the war be divided into?, Feb. 25, 2023, Accessed: Aug. 31, 2023. [Online]. Available: https://tech.ifeng.com/c/8NhD66vPRNv
[23] X. Li, Y. Zhou, M. Zhao, and X. Zhao, "A harmonized global nighttime light dataset 1992–2018," *Sci. Data*, vol. 7, no. 1, Jun. 2020, Art. no. 168, doi: 10.1038/s41597-020-0510-y.
[24] P. Xu, Q. Wang, J. Jin, and P. Jin, "An increase in nighttime light detected for protected areas in mainland China based on VIIRS DNB data," *Ecol. Indicators*, vol. 107, Dec. 2019, Art. no. 105615, doi: 10.1016/j.ecolind.2019.105615.
[25] H. Mahdi and T. Hebib, "Mediterranean sea level trends from long-period tide gauge time series," *Acta Oceanol. Sinica*, vol. 39, no. 1, pp. 157–165, Jan. 2020, doi: 10.1007/s13131-020-1532-1.
[26] X. Li, L. Ge, and X. Chen, "Detecting Zimbabwe's decadal economic decline using nghttime light imagery," *Remote Sens.*, vol. 5, no. 9, pp. 4551–4570, Sep. 2013, doi: 10.3390/rs5094551.
[27] S. Conner, "Ukraine Crisis: The search for safety," medair.org, 2022. Accessed: Nov. 3, 2023. [Online]. Available: https://www.medair.org/stories/Ukraine-crisis-the-search-for-safety/
[28] "Ukrainians face long journeys to borders as fighting escalates," Reuters, economictimes.indiatimes.com, 2022. Accessed: Nov. 3, 2023. [Online]. Available: https://economictimes.indiatimes.com/news/international/world-news/ukrainians-face-long-journeys-to-borders-as-fighting-escalates/articleshow/89929511.cms
[29] "Curfew in Regions of Ukraine," visitukraine.today, 2022. Accessed: Nov. 3, 2023. [Online]. Available: https://visitukraine.today/blog/97/curfew-in-the-regions-of-Ukraine-updatedv
[30] H. L. Jullian, "Ukraine–Russia negotiators agree on humanitarian corridor for civilians," jewishpress.com, 2022. Accessed: Aug. 31, 2023. [Online]. Available: https://www.jewishpress.com/news/global/Europe/Ukraine/Ukraine-Russia-negotiators-agree-on-humanitarian-corridor-for-civilians/2022/03/03/
[31] "Ukraine: Locals, foreign students flee through 'humanitarian corridors' but Kyiv says Russia shelled an evacuation route," Reuters, scmp.com, 2022. Accessed: Aug. 31, 2023. [Online]. Available: https://www.scmp.com/news/world/Europe/article/3169730/ukrainians-flee-some-besieged-areas-through-humanitarian
[32] M. Bachelet, "Update to the Human Rights Council on Ukraine," Ohchr.org, 2022. Accessed: Aug. 31, 2023. [Online]. Available: https://www.ohchr.org/en/statements/2022/03/update-human-rights-council-Ukraine
[33] "Despite ongoing war and lack of access to care, many refugees return to Ukraine," who.int, 2022. Accessed: Aug. 31, 2023. [Online]. Available: https://www.who.int/Europe/news/item/16-08-2022-despite-ongoing-war-and-lack-of-access-to-care--many-refugees-return-to-Ukraine
[34] B. Chappell, "100 Days after Ukraine was plunged into war, over 2 million Ukrainians have returned," npr.org, 2022. Accessed: Aug. 31, 2023. [Online]. Available: https://www.npr.org/2022/06/03/1102935668/Russia-Ukraine-war-100-days-refugees-ukrainians-return
[35] A. P Le Monde with, "Russia hits power stations after Ukraine counter-offensive," lemonde.fr, 2022. Accessed: Aug. 31, 2023. [Online]. Available: https://www.lemonde.fr/en/international/article/2022/09/12/Russia-hits-power-stations-after-Ukraine-counteroffensive_5996571_4.html
[36] "'Wide-scale' Russian attacks target Ukraine's energy grid, leaving millions without electricity," RFE/RL's Ukrainian Service, jewishpress.com, 2022. Accessed: Aug. 31, 2023. [Online]. Available: https://www.rferl.org/a/Ukraine-russian-attacks-energy-grid-electricity/32096876.html

Lin Wang received the Ph.D. degree in remote sensing of environment and resource from the Fuzhou University, Fuzhou, China, in 2018.

He is currently an Associate Professor with the College of Environment and Safety Engineering, Fuzhou University. His research interests include feature extraction from satellite imagery and nighttime light remote sensing technology.

Henggang Lei received the bachelor's degree in geographic country monitoring from the Wuhan University, Wuhan, China, in 2021. He is currently working toward the master's degree in geomatics engineering with the Academy of Digital China (Fujian), Fuzhou University, Fuzhou, China.

His research interests include feature extraction from satellite imagery and nighttime light remote sensing technology.

Hanqiu Xu received the Ph.D. degree in earth sciences from the National University of Ireland, Cork, Ireland, in 1996.

He is currently a Professor with the College of Environment and Safety Engineering, Fuzhou University, Fuzhou, China. He has authored and coauthored more than 200 peer-reviewed papers. His research interests include remote sensing of urban thermal environment and feature extraction from satellite imagery.